Calibrated Two-Port Microwave Measurement up to 26.5 GHz for Wide Temperature Range From 4 to 300 K

Tomonori Arakawa, *Member, IEEE*, and Seitaro Kon, *Member, IEEE*

***Abstract*— To realize a quantum information processing system, it is necessary not only to increase the number of physical qubits but also to cooperatively operate a multitude of cryogenic microwave components, such as cables, circulators, and amplifiers for controlling or reading them. Therefore, it is essential to develop metrological methods to precisely evaluate the microwave scattering parameters of each component at low temperatures. Here, we report a calibrated microwave measurement method for a wide temperature range of 4–300 K. At each temperature, we performed a full two-port calibration, which enables us to precisely measure the scattering parameters of various cryogenic microwave components up to 26.5 GHz by using 3.5-mm connectors as the reference planes. We carefully verified the validity of the calibration impedance elements and demonstrated our method by evaluating the temperature-dependent characteristics of a coaxial cable and a circulator.**

***Index Terms*— Coaxial components, cryogenics, microwave measurement, short–open–load–thru (SOLT) calibration, unknown thru, vector network analyzer (VNA).**

I. Introduction

RECENTLY, rapid progress has been made in the development of quantum computers, as the number of physical qubits continues to increase [1]. To accelerate this development and realize a million-qubit quantum computer, it is crucial to develop not only qubits but also cryogenic microwave circuits to control them [2], [3]. However, most microwave components and evaluation methods are designed for using at room temperature, and the commercially available components for cryogenic applications are limited. The development of cryogenic components must be accelerated to realize advanced quantum information systems. An important issue is the establishment of calibration methods to evaluate the microwave scattering parameters (S-parameters) of each component at the temperatures under which they will be used. The S-parameters of each component depend on the temperature and can cause a decrease in the fidelity of qubits, when multiple microwave components are operated in collaboration [4].

Several calibration methods have been proposed to characterize a device under test (DUT) at low temperatures using a vector network analyzer (VNA) at room temperature. Microwave switches are commonly used to exchange a set of well-known standards (STs), and the DUT in a cryostat to determine the microwave response of the measurement lines and obtain the S-parameters of the DUT alone. One-port calibration methods for coaxial components have been realized using a short–open–load (SOL) calibration procedure, in which three well-known impedance STs are used [4], [5]. By extending this method, a two-port short–open–load–thru (SOLT) calibration procedure with an unknown thru was realized [6]. A thru–reflect–line (TRL) calibration procedure has also been used to measure the two-port S-parameters of coaxial components and planar waveguides [7], [8]. Such calibration methods have been demonstrated at millikelvin temperatures by placing DUTs in the lowest temperature stage of a dilution refrigerator. However, in quantum computing systems, a variety of cryogenic microwave components, such as circulators, filters, coaxial cables, and amplifiers, are placed at several different temperature stages. Manufacturers must evaluate components at various temperatures to accelerate the integration and advancement of cryogenic microwave circuits. More importantly, in the development of new cryogenic components, it is important to accurately determine the S-parameters as a function of temperature and feed them back into the circuit design because material parameters, such as permittivity, permeability, and resistivity, exhibit different temperature dependences. Thus, a calibrated microwave measurement method over a wide temperature range can contribute to the supply chain of cryogenic microwave components.

In this article, we present a measurement method over a wide temperature range of 4–300 K based on the SOLT calibration procedure using two microwave switches and an unknown thru [9]. To achieve a wide temperature range and flexibility in the port configuration of the DUT, we developed a measurement system in a custom refrigerator with a mechanical heat switch. This system enabled us to precisely measure the temperature dependence of the S-parameters of various cryogenic microwave components up to 26.5 GHz with reference to a well-defined 3.5-mm connectors plane. The uncertainties in the temperature dependence of the impedance STs were discussed based on the experimental results. Finally,

Manuscript received 27 July 2023; revised 24 August 2023; accepted 29 August 2023. Date of publication 14 September 2023; date of current version 4 October 2023. This work was supported by the Japan Society for the Promotion of Science (JSPS) KAKENHI under Grant JP22H01964 and Grant JP22H01936. The Associate Editor coordinating the review process was Dr. Yang Bai. *(Corresponding author: Tomonori Arakawa.)*

The authors are with the National Metrology Institute of Japan, National Institute of Advanced Industrial Science and Technology, Tsukuba 305-8563, Japan (e-mail: tomonori-arakawa@aist.go.jp).

Digital Object Identifier 10.1109/TIM.2023.3315393

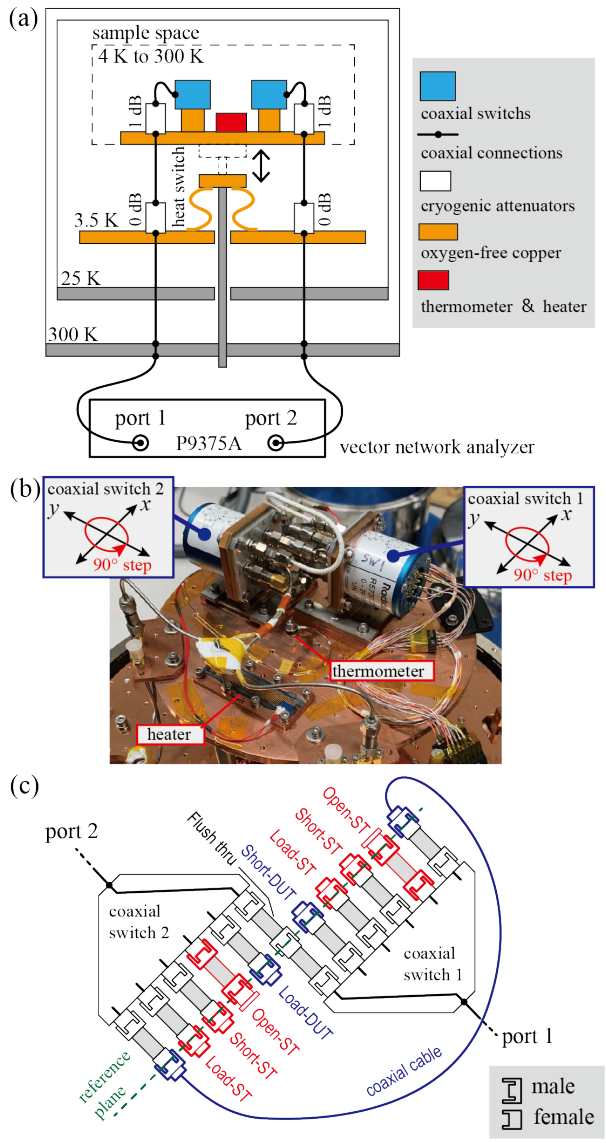

Fig. 1. (a) Schematic of the measurement system. (b) Photograph on the sample space. Schematics in the blue box represent the degree of freedom in the microwave switch placement. (c) Experimental schematic of the two-port S-parameter measurement.

we demonstrate the proposed method by evaluating a coaxial cable and a circulator.

II. Experimental Setup

Because the sample space of commercially available variable temperature refrigerators is not sufficiently large to place the microwave switches and DUTs, we developed a custom-made refrigerator using a two-stage Gifford-McMahon Cryocooler unit with a cooling power of 1.5 W at 4.2 K (SHI Cryogenics Group RDK-415D). Fig. 1(a) shows a schematic of the measurement system. The refrigerator consists of four stages, and the heat conduction between the top sample stage and the 3.5-K stage with the lowest temperature can be controlled by a mechanical heat switch. As a result, the temperature of the sample stage could be tuned over a wide temperature range of 4–300 K using a calibrated resistance thermometer (Lake Shore Cryotronics CX-1030-CU-HT-1.4L)

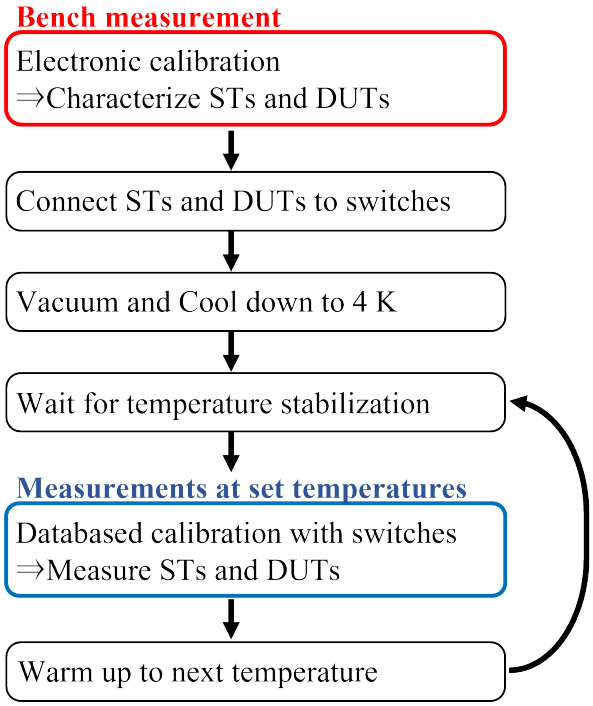

Fig. 2. Conceptual map for the calibration procedure.

and a film heater (maximum power, 50 W), where the heat switch was disconnected at temperatures above 50 K. Two coaxial lines from a room-temperature VNA (Keysight P9375A) were connected to two microwave switches on the sample stage, where attenuators were inserted to thermally connect the inner conductors of the coaxial lines. In this study, the S-parameters were measured in the frequency range of 2 MHz–26.5 GHz with 13 250 points using a source power of 0 dBm and an intermediate frequency (IF) bandwidth of 1 kHz.

Fig. 1(b) shows a photograph of the sample stage. The calibration STs and DUTs were connected to each port of the single pole six-throw microwave switches (Radiall R573F22600), with the thermometer and heater located in their vicinity. These switches were pressed onto a sample stage made of oxygen-free copper with a diameter of 200 mm and thickness of 6 mm to ensure sufficient thermal contact. As schematically shown by the blue boxes in Fig. 1(b), each microwave switch can be continuously moved in the xy plane and rotated at 90° intervals to accommodate DUTs with various port configurations. The measurement setup is illustrated in Fig. 1(c). Here, each ST and DUT were connected via APC-3.5-mm adapters (KPC350 Series, Kawashima Manufacturing Company) [10]. Thus, after calibration, the reference plane was a dielectric-free coaxial connector, and the temperature dependence of the characteristic impedance of the reference plane was minimized. In addition, two types of adapters with the same electrical length were available: male-to-female (KPC350MF) and male-to-male (KPC350MM). By using these adapters appropriately, our calibration method does not depend on the gender of the DUT port. More importantly, we can

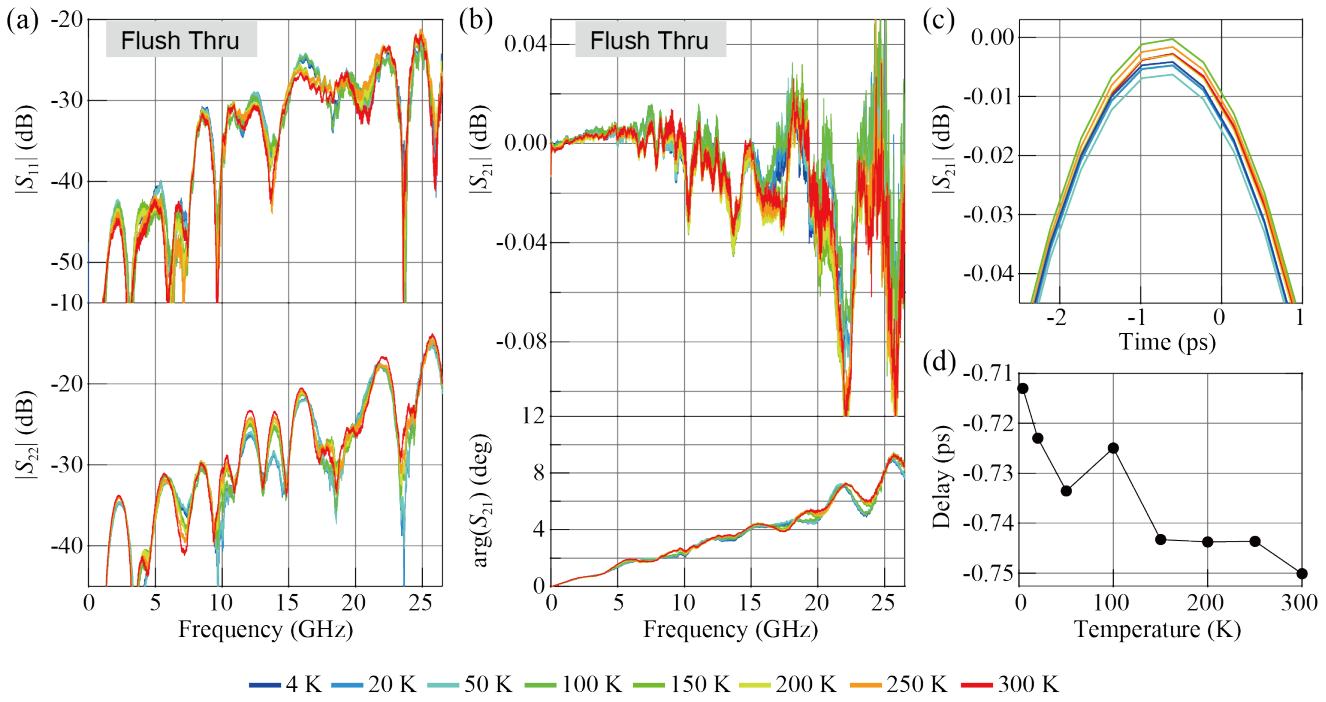

Fig. 3. Results of S-parameter measurement and time-domain analysis for flush thru at several temperatures. (a) Amplitude of the reflection coefficients measured at both ports. (b) Amplitude and phase components of the measured transmission coefficients. (c) Time-domain response of the transmission coefficients. (d) Delay time is estimated from (c) as a function of temperature.

realize "flush thru," a transmission line with zero electric length, which enables us to estimate the uncertainties of the S-parameter measurement.

III. Calibration Procedure and Impedance Elements

As shown in Fig. 2, the present calibration procedure was performed using the following steps based on previously reported methods [4], [5], [6]. First, the impedance elements were characterized at room temperature using a conventional method without microwave switches. The VNA was calibrated using an electronic calibration kit (Keysight N4691B) [11], and the S-parameters of open-STs, short-STs, and load-STs were measured to define two sets of databased-calibration kits, as detailed in the Appendix. This conventional method, referred to as bench measurement in this study, was also used to characterize the DUTs. Next, we connected the STs and DUTs to the microwave switches via adapters on the sample stage and cooled the system to the lowest temperature (4 K). Third, after the temperature stabilized, we waited for at least 1 h, and then, the SOLT calibration was performed with the database calibration kits and an unknown thru, using the microwave switches as needed [12], [13]. In the present setup shown in Fig. 1(c), the flush thru and coaxial cable are available as the unknown thru, but the influence of this choice on the calibration results is negligible. Fourth, all components, including STs, were measured using the calibrated system. We then set the sample stage to the next temperature and repeat the third and fourth steps.

In cryogenic calibration methods, the S-parameters of STs are characterized at room temperature, assuming that they are independent of temperature [4], [5], [6]. Therefore, it is important to select STs with small temperature variations and commercially available STs are not suitable. In Sections III-A–III-C, we describe the specifications of the prepared STs and DUTs.

A. Short Elements

An offset short is commonly used for calibration methods at room temperature, where the transmission line between the reference and conducting planes is described by the offset characteristic impedance, offset delay, and offset loss [14]. Although the offset is important for achieving both well-defined open and short STs with the same electric length, the offset parameters apparently depend on the temperature owing to the variation in conductivity. Therefore, a zero-offset short circuit with the conductor surface placed on the reference plane may be the best choice for calibration at low temperatures. The only temperature-dependent factor was the conducting plane. To confirm this effect, we prepared two types of zero-offset shorts with different temperature dependences of conductivity: a short-ST made of passivated steel and a short-DUT made of gold-plated brass.

B. Open Elements

From the perspective of temperature-independent calibration, a zero-offset open with an open end on the reference plane is desirable. The simplest method involves a direct connection of a dust cap to a female connector. Here, the inner pin of the male-to-female adapter is used for the open

end, which makes it difficult to apply as a well-defined calibration element because the pin shape depends on the manufacturer. In addition, the dust cap exhibited a phase shift of approximately 30° at 26.5 GHz in the bench measurement, as shown in the Appendix. This could be problematic because the relative phase difference between the open and short STs at a given frequency should be 180°; otherwise, the resulting calibration accuracy is reduced around a specific phase [12]. Therefore, a custom adapter with a truncated conical inner pin at the open end was prepared, and open-ST was defined as a set of this adapter and dust cap, as shown in Fig. 1(c).

C. Load Elements

We prepared two types of commercially available cryogenic terminations: load-ST and load-DUT, which are offset loads with female connectors of 2.92 mm and sub-miniature type A (SMA), respectively. Here, they have different offset lengths, and their phase characteristics have significant differences, as shown in the Appendix. This is an important feature to evaluate the temperature dependence of the termination itself. In other words, if their reflection coefficients and temperature dependence are identical, their respective temperature variations cancel out and not be detected.

IV. Calibration Results and Verification

We begin with a description of the measurement results for flush thru, which is a zero-length connection between ports 1 and 2. In this connection, unknown parameters in the actual S-parameters were eliminated, allowing us to directly evaluate the accuracy of the present SOLT calibration method. Fig. 3(a) shows the frequency dependence of the measured reflection magnitudes ($|S_{11}|$ and $|S_{22}|$) at several temperatures. Because the reflections depend on the port, they are aligned vertically and displayed in different vertical ranges. Although the undesired reflections increased for both ports with increasing frequency, the variation due to the temperature change was not significant. Consequently, we achieved sensitivities of approximately 30 dB up to 10 GHz and 20 dB up to 20 GHz, regardless of the measurement temperature and connector gender. This sensitivity is sufficient to characterize the impedance matching of the microwave components used in quantum computers, where impedance mismatch reduces the fidelity of qubit operations [4], [6]. Finally, we discuss the differences between ports 1 and 2. The reflection magnitude for port 2 was slightly larger over the entire frequency range, probably because the STs worked more accurately with respect to the female terminal at port 1. In other words, only the male terminal of the electronic calibration kit was used to obtain the data-based responses of the STs, as shown in the Appendix.

We discuss the transmission characteristics based on the measured frequency dependence at several temperatures, as shown in Fig. 3(b). For the flush thru, the transmission magnitude $|S_{21}|$ is expected to be 0 dB, and each measured $|S_{21}|$ fluctuates around 0 dB as a function of frequency. The resulting error increases with frequency, approximately

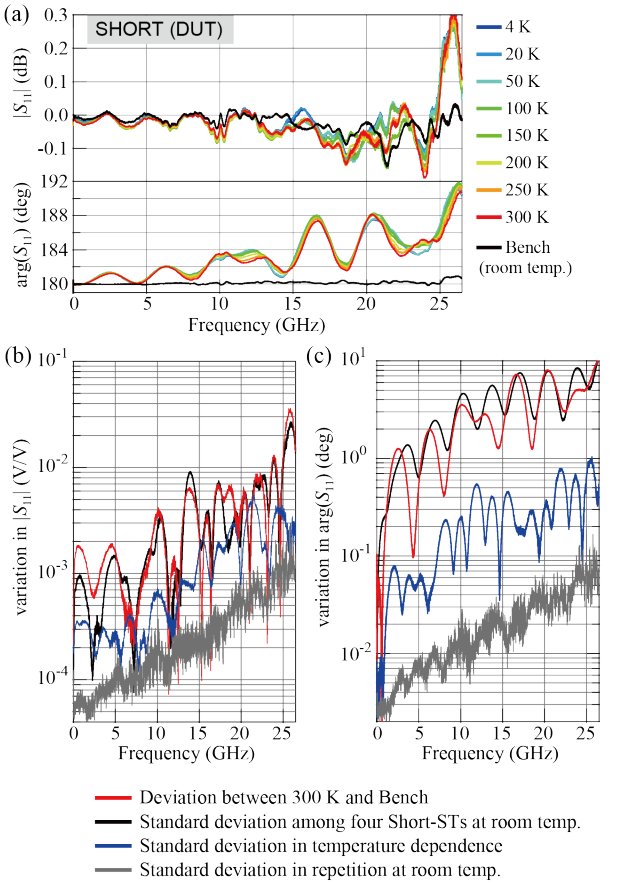

Fig. 4. (a) Amplitude and phase components of the reflection coefficients for short-DUT. The black and colored lines correspond to the bench measurement and the results at each temperature, respectively. (b) and (c) Estimated deviations in the amplitude and phase measurements, respectively.

±0.04 dB at 10 GHz and ±0.06 dB at 20 GHz, which is comparable to the previous method by using an SOL calibration procedure and time gating technique [4]. More importantly, the measured $|S_{21}|$ is highly stable with respect to the set temperature, exhibiting a relative variation within ±0.01 dB at 10 GHz and ±0.03 dB at 20 GHz. The measured phase component arg(S_{21}) increases almost linearly with the frequency, indicating that the electric length offset dominated the error. To investigate this in detail, the results in Fig. 3(b) were converted using a time-domain analysis, and the resulting impulse responses are shown in Fig. 3(c). Although no delay is expected for flush thru, each delay estimated from the peak position is about −0.7 ps, which corresponds to an error of −0.2 mm in electrical length. Fig. 3(d) shows the estimated delay as a function of the measurement temperature. The relative error depended slightly on the temperature, but its variation is below 0.04 ps. This means that temperature-dependent changes in the electrical length can be detected with an accuracy of several tens of micrometers.

The error sources in the proposed SOLT calibration procedure can be classified into two types. The first is a temperature-independent systematic error, and the other is a relative error in the temperature dependence. In the following, these error factors are discussed based on the measurement results for short- and load-DUT.

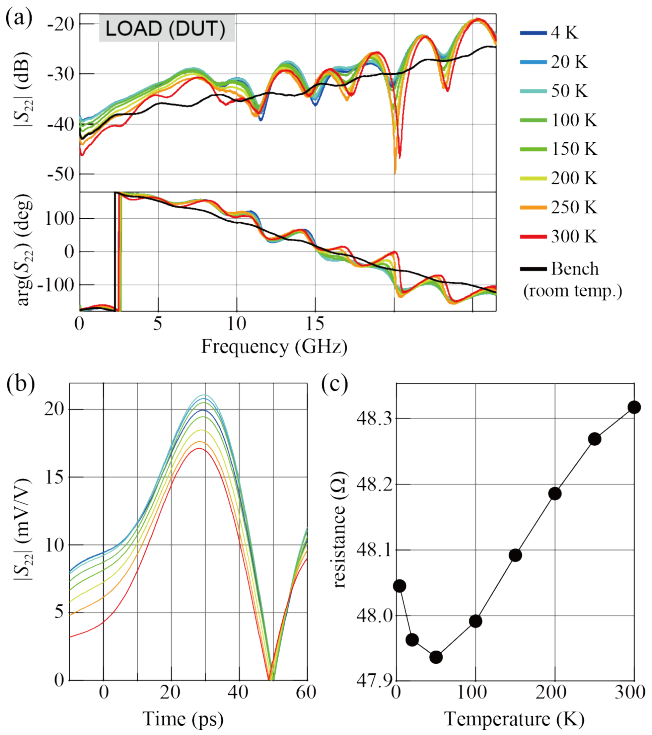

Fig. 5. (a) Amplitude and phase components of the reflection coefficients for load-DUT. The black and colored lines correspond to the bench measurement and the results at each temperature, respectively. (b) Time-domain response of the reflection coefficients at each temperature. (c) Resistance is estimated from the peak heights in (b) as a function of temperature.

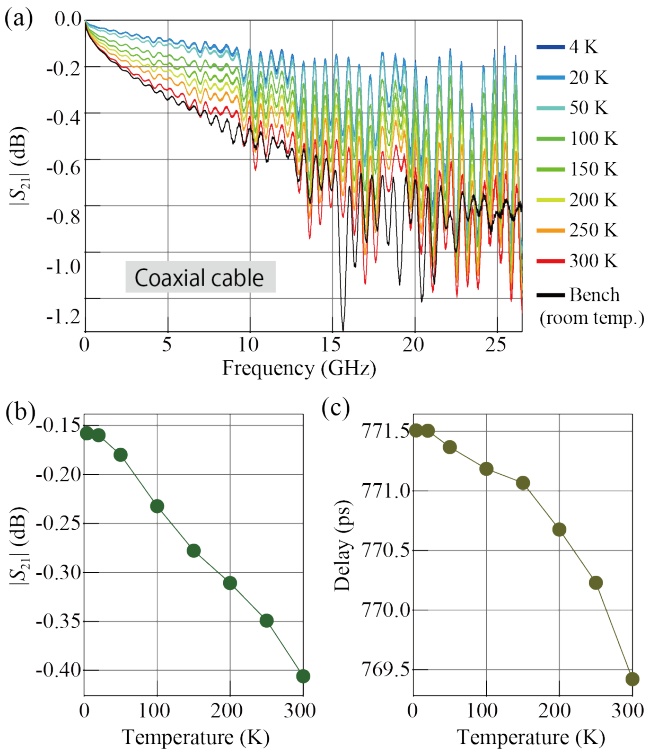

Fig. 6. (a) Measured transmission amplitude of the coaxial cable at several temperatures. The black line corresponds to the bench measurement. (b) and (c) Estimated amplitude and delay time as a function of temperature, respectively.

A. Short-DUT

Fig. 4(a) shows the measured reflection coefficients for short-DUT. Comparing the frequency dependence at each temperature with the bench results, the systematic errors in magnitude $|S_{11}|$ and phase $\arg(S_{11})$ are comparable to those in $|S_{21}|$ and $\arg(S_{21})$ in Fig. 3(b), respectively. The relative error also shows similar behavior to the results for the flush thru, and there is no clear correlation with the measurement temperature. Because the measured $|S_{11}|$, which reflects the relative difference between short-DUT and short-ST, is expected to decrease monotonically with temperature, we conclude that the temperature variation of a zero-offset short is not the dominant error factor in the calibration method.

To identify the origin of these errors, the deviations between the microwave switch ports and the repeatability of each port were evaluated at room temperature. Here, instead of the short-DUT, flush thru, and coaxial cable, three additional short-STs were connected to switch 1 to estimate the deviations between switch positions under the same conditions. In Fig. 4(b) and (c), we compare several types of deviations in the $|S_{11}|$ and $\arg(S_{11})$ measurements. The deviation between the 300 K and bench measurements was in good agreement with the ST deviation among the four short-ST measurements, indicating that the main source of the temperature-independent systematic error was the variation between the transmission paths from the common port of the microwave switch to the reference plane. This variation is attributed to the microwave switch, as shown in the Appendix.

On the other hand, the ST deviation in the temperature dependence for short-DUT measurements is approximately an order of magnitude smaller than the systematic error. Although this relative error could be caused by the repeatability of the switching operation, the ST deviation for a single short-ST at room temperature is so small that it is comparable to the noise floor of the VNA. This implies that the stability of the mechanical switching operation decreases at low temperatures [5].

B. Load-DUT

Fig. 5(a) shows the measured reflection coefficients for the load-DUT, where the data for each temperature and bench measurement are plotted. Unlike the results for short-DUT, the reflection magnitude $|S_{22}|$ varied monotonically with respect to temperature. Although this variation was smaller than the deviation from the bench measurement resulting from the microwave switch, the temperature dependence of the load ST could be a major source of error. To quantitatively investigate the temperature variation, the measurement results in Fig. 5(a) were converted into impulse responses, as shown in Fig. 5(b), where each peak at approximately 30 ps represents the reflection by a resistor. Generally, the reflection coefficient at a resistor (R Ω) connected to a waveguide with a characteristic impedance ($Z_0 = 50$ Ω) is given by $(R - Z_0)/(R + Z_0)$. Although the measured $|S_{22}|$ depends on the temperature variation of the load-ST, this equation allows us to roughly calculate the change in resistance. Fig. 5(c) shows the resistance estimated from the peak height as a

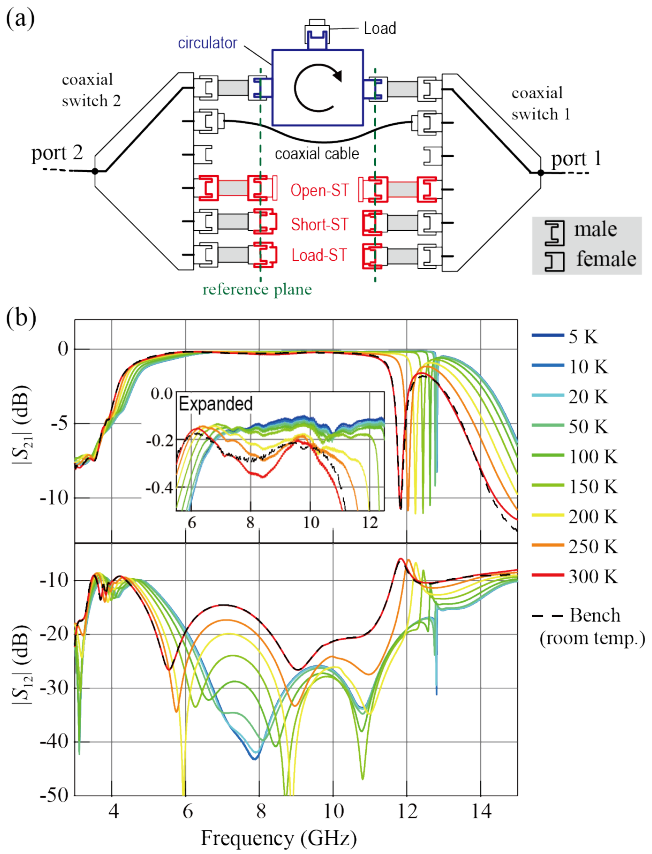

Fig. 7. (a) Experimental schematic of the two-port S-parameter measurement for a circulator. (b) Measured transmission amplitude of the circulator at several temperatures. Black dashed lines correspond to the bench measurement.

function of the measured temperature. As the temperature decreased, the resistance decreased monotonically, reached a local minimum at 50 K, and then increased. In general, the conductivity of a conductor decreases with temperature because of reduced phonon scattering and then saturates by defect scattering. One possible mechanism for the local minimum in conductivity at 50 K is the Kondo effect [15].

V. Application

To demonstrate the practicality of the calibrated measurement method, we measured the temperature dependence of the S-parameters of a coaxial cable and a circulator.

An economical semiflexible coaxial cable, consisting of an outer diameter of 2.15 mm and a length of 15 cm or less, with male SMA connectors at both ends, was measured under the same cooling, as shown in Fig. 1(c). Fig. 6(a) shows the measured transmission amplitude $|S_{21}|$ at several temperatures in addition to the bench measurement. The measured $|S_{21}|$, the so-called insertion loss, decreases with decreasing temperature. The fine oscillations in each frequency dependence were owing to standing waves caused by reflections at both ends of the coaxial cable, which could be a problem in qubit manipulation [16]. Note that the deviation between the 300 K and bench result was mainly due to the bending of the cable. To characterize the temperature dependence of the cable, the measured transmission characteristics were converted to

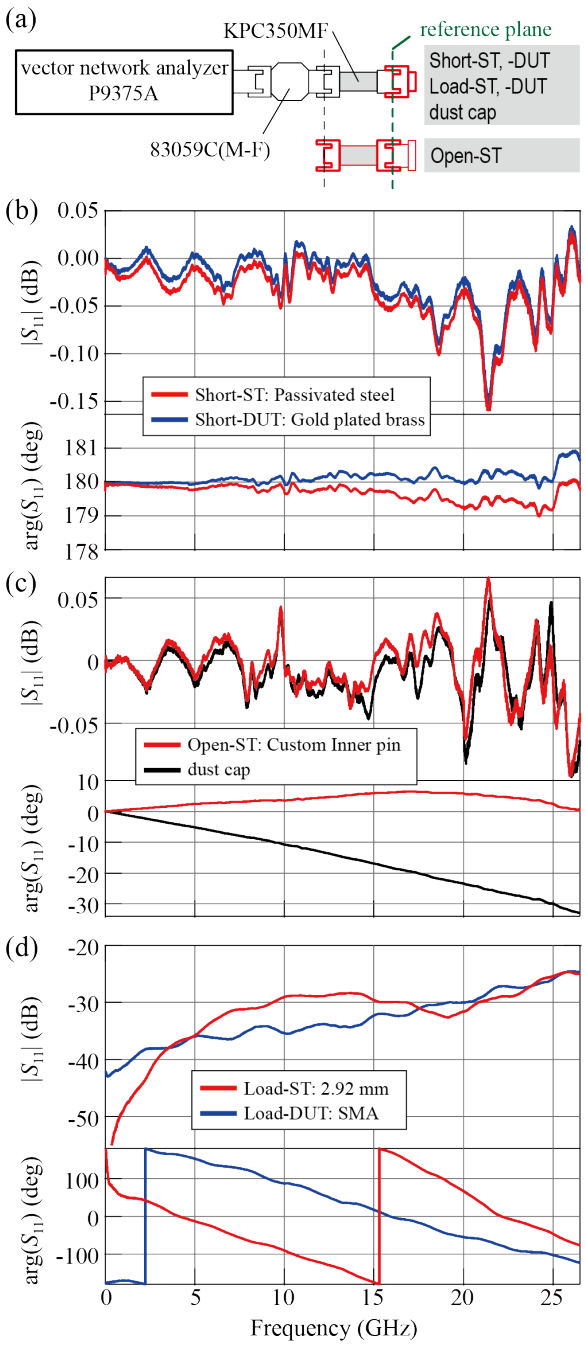

Fig. 8. (a) Experimental schematic of the bench measurement. (b)–(d) Amplitude and phase components of the measured reflection coefficients for short, open, and load elements, respectively.

impulse responses, and we estimated the amplitude and delay times as functions of temperature, as shown in Fig. 6(b) and (c), respectively. With decreasing temperature, the insertion loss decreases monotonically, reflecting an increase in conductivity. However, the delay time increases monotonically with cooling, probably because of an increase in the dielectric constant. Note that both temperature variations saturate at approximately 20 K, indicating that the properties of cryogenic components at millikelvin temperatures can be predicted from their temperature dependence, except in special cases such as superconducting transitions.

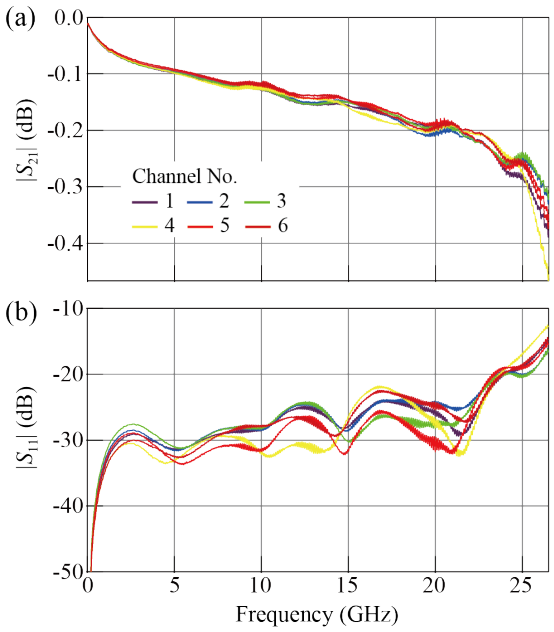

Fig. 9. (a) and (b) Measured transmission and reflection amplitude for each channel of the microwave switch 1, respectively.

To measure the cryogenic circulator, we changed the setup as shown in Fig. 7(a) and performed another cooling process. The coaxial cable operates as an unknown thru, and the third port of the circulator is terminated with a cryogenic load. Fig. 7(b) shows the measured insertion losses $|S_{21}|$ and isolation $|S_{12}|$ at several temperatures, in addition to the bench measurements. The good agreement between the 300 K and bench results indicates that the proposed calibration method worked correctly. With decreasing temperature, the operating frequency range of the circulator shifted toward the high-frequency side. Simultaneously, the magnitude of the isolation changed significantly, and the insertion loss decreased monotonically, as shown in the inset of Fig. 7(b). These results imply that the temperature dependence of material parameters, such as permittivity and permeability, must be considered when developing a high-performance circulator at a given temperature.

VI. Conclusion

We presented a calibrated microwave measurement method for a wide temperature range of 4–300 K. To achieve a wide temperature range and flexibility of the DUT, a measurement system was developed on a custom refrigerator, and the SOLT calibration procedure was performed at the given temperature. We evaluated and demonstrated the performance of our system by measuring several DUTs, including a zero-length connection, impedance elements, coaxial cables, and circulators. Consequently, we achieved an accurate measurement scheme regardless of the measurement temperature and connector gender of the DUT.

Information on the continuous temperature dependence from room temperature is essential for the optimization process to develop new cryogenic components. Our method provides a more efficient development process and contributes not only to the realization of quantum computers but also to advancements in astrophysical observations and condensed matter physics. On the other hand, it is important to standardize the cryogenic S-parameter measurement methods to accelerate the development of cryogenic components and realize a quantum information processing system. In this study, we performed a two-port calibration with well-defined 3.5-mm connectors as reference planes and investigated the origins of errors. The findings of this study contribute to standardization.

Appendix

The experimental setup for the bench measurements is schematically shown in Fig. 8(a), where a usual one-port calibration with Keysight N4691B was performed at the end of the KPC350MF adapter connected via a high-quality 3.5-mm adapter (Keysight 83059C). Fig. 8(b) shows the frequency dependence of the reflection coefficients of short-ST and short-DUT. Short-ST exhibited slightly lossy behavior and smaller values in $|S_{11}|$, which was expected from its lower conductivity. The frequency dependence of the $\arg(S_{11})$ in both elements is extremely flat within $180° \pm 1°$ up to 26.5 GHz, indicating that the reference plane and the conductor plane are in the same position. Fig. 8(c) shows the frequency dependence of the reflection coefficients of Open-ST and the dust cap. While the difference in magnitude $|S_{11}|$ is almost negligible between open-ST and the dust cap, there is a significant difference in phase $\arg(S_{11})$. For open-ST, the measured $\arg(S_{11})$ shifted by only 7°, allowing fine calibration up to 26.5 GHz. Fig. 8(d) shows the reflection coefficients of load-ST and load-DUT. Although the reflection magnitude $|S_{11}|$ is large compared with high-quality broadband loads with impedance matching below −40 dB, this is not a critical problem because the database calibration uses actual measured data.

We also characterized the microwave switch alone using the usual two-port calibration with Keysight N4691B. Fig. 9(a) and (b) shows the channel dependences of the transmission and reflection amplitudes, respectively, for microwave switch 1. The measured variation dominated the error in the calibration method.

Acknowledgment

The authors would like to thank S. Singh, N.-H. Kaneko, M. Horibe, S. Tamaru, K. Inomata, and T. Ishikawa for their valuable discussions.

References

[1] F. Arute et al., "Quantum supremacy using a programmable superconducting processor," *Nature*, vol. 574, no. 7779, pp. 505–510, Oct. 2019, doi: 10.1038/s41586-019-1666-5.

[2] P. Krantz, M. Kjaergaard, F. Yan, T. P. Orlando, S. Gustavsson, and W. D. Oliver, "A quantum engineer's guide to superconducting qubits," *Appl. Phys. Rev.*, vol. 6, no. 2, Jun. 2019, Art. no. 021318, doi: 10.1063/1.5089550.

[3] J. C. Bardin, D. H. Slichter, and D. J. Reilly, "Microwaves in quantum computing," *IEEE J. Microw.*, vol. 1, no. 1, pp. 403–427, Jan. 2021, doi: 10.1109/JMW.2020.3034071.

[4] S. Simbierowicz, V. Y. Monarkha, S. Singh, N. Messaoudi, P. Krantz, and R. E. Lake, "Microwave calibration of qubit drive line components at millikelvin temperatures," *Appl. Phys. Lett.*, vol. 120, no. 5, Feb. 2022, Art. no. 054004, doi: 10.1063/5.0081861.

[5] H. Wang et al., "Cryogenic single-port calibration for superconducting microwave resonator measurements," *Quantum Sci. Technol.*, vol. 6, no. 3, Jun. 2021, Art. no. 035015, doi: 10.1088/2058-9565/ac070e.
[6] S. Simbierowicz, V. Y. Monarkha, M. von Soosten, S. Andresen, and R. E. Lake, "Calibrated transmission and reflection from a multi-qubit microwave package," *Rev. Sci. Instrum.*, vol. 94, no. 5, May 2023, Art. no. 054713, doi: 10.1063/5.0144840.
[7] L. Ranzani, L. Spietz, Z. Popovic, and J. Aumentado, "Two-port microwave calibration at millikelvin temperatures," *Rev. Sci. Instrum.*, vol. 84, no. 3, Mar. 2013, Art. no. 034704, doi: 10.1063/1.4794910.
[8] M. Stanley, R. Parker-Jervis, S. de Graaf, T. Lindström, J. E. Cunningham, and N. M. Ridler, "Validating S-parameter measurements of RF integrated circuits at milli-Kelvin temperatures," *Electron. Lett.*, vol. 58, no. 16, pp. 614–616, Jun. 2022, doi: 10.1049/ell2.12545.
[9] K. Wong, "The 'unknown thru' calibration advantage," in *Proc. ARFTG 63rd Conf.*, Fort Worth, TX, USA, 2004, pp. 73–81, doi: 10.1109/ARFTG.2004.1387858.
[10] *IEEE Standard for Precision Coaxial Connectors (DC to 110 GHz)*, IEEE Standard 287–2007 (Revision of IEEE Standard 287–1968), pp. 1–142, Sep. 2007, doi: 10.1109/IEEESTD.2007.4317507.
[11] J. A. Jargon, D. F. Williams, T. M. Wallis, D. X. LeGolvan, and P. D. Hale, "Establishing traceability of an electronic calibration unit using the NIST microwave uncertainty framework," in *Proc. 79th ARFTG Microw. Meas. Conf.*, Montreal, QC, Canada, 2012, pp. 1–5, doi: 10.1109/ARFTG79.2012.6291181.
[12] B. Bianco, A. Corana, S. Ridella, and C. Simicich, "Evaluation of errors in calibration procedures for measurements of reflection coefficient," *IEEE Trans. Instrum. Meas.*, vol. IM-27, no. 4, pp. 354–358, Dec. 1978, doi: 10.1109/TIM.1978.4314711.
[13] A. Ferrero and U. Pisani, "Two-port network analyzer calibration using an unknown 'thru,"' *IEEE Microw. Guided Wave Lett.*, vol. 2, no. 12, pp. 505–507, Dec. 1992, doi: 10.1109/75.173410.
[14] J.-S. Kang, J.-H. Kim, and D.-C. Kim, "Phase analysis of coaxial short and open circuits," *IEEE Trans. Instrum. Meas.*, vol. 54, no. 2, pp. 701–704, Apr. 2005, doi: 10.1109/TIM.2004.843335.
[15] J. Kondo, "Resistance minimum in dilute magnetic alloys," *Prog. Theor. Phys.*, vol. 32, no. 1, pp. 37–49, Jul. 1964, doi: 10.1143/PTP.32.37.
[16] S. Gustavsson et al., "Improving quantum gate fidelities by using a qubit to measure microwave pulse distortions," *Phys. Rev. Lett.*, vol. 110, no. 4, Jan. 2013, Art. no. 040502, doi: 10.1103/PhysRevLett.110.040502.

Tomonori Arakawa (Member, IEEE) received the B.E. degree in applied physics from Kyoto University, Kyoto, Japan, in 2009, the M.E. degree from the Kyoto University of Advanced Science, Kyoto, in 2011, and the Ph.D. degree in science from Kyoto University, in 2014.

Then, he became an Assistant Professor with the Graduate School of Science, Osaka University, Suita, Japan. He moved to the National Institute of Advanced Industrial Science and Technology (AIST), Tokyo, Japan, in 2021, where he is currently working as a Researcher in the field of instrumentation at microwave, condensed matter physics, and electron/spin dynamics.

Seitaro Kon (Member, IEEE) received the B.S. degree in physics from the Tokyo University of Science, Tokyo, Japan, in 2005, the M.S. degree in environmental science from Tsukuba University, Tsukuba, Japan, in 2007, and the Ph.D. degree in engineering from Shinshu University, Nagano, Japan, in 2014.

He joined the National Metrology Institute of Japan, National Institute of Advanced Industrial Science and Technology (AIST), Tsukuba, in 2007, as a Research Scientist. He has been involved in highly precise current, impedance, and power measurements, and in the development of sensor applications using RF, microwaves, and millimeter waves.